



**HAL**  
open science

## **Functional rescue of an ABCB11 mutant by ivacaftor: A new targeted pharmacotherapy approach in bile salt export pump deficiency**

Elodie Mareux, Martine Lapalus, Rachida Amzal, Marion Almes, Tounsia Aït-slimane, Jean-louis Delaunay, Pauline Adnot, Mauricette Collado-Hilly, Anne Davit-spraul, Thomas Falguières, et al.

### ► To cite this version:

Elodie Mareux, Martine Lapalus, Rachida Amzal, Marion Almes, Tounsia Aït-slimane, et al.. Functional rescue of an ABCB11 mutant by ivacaftor: A new targeted pharmacotherapy approach in bile salt export pump deficiency. *Liver International*, 2020, 40 (8), pp.1917-1925. 10.1111/liv.14518 . hal-04001111

**HAL Id: hal-04001111**

**<https://hal.science/hal-04001111>**

Submitted on 22 Feb 2023

**HAL** is a multi-disciplinary open access archive for the deposit and dissemination of scientific research documents, whether they are published or not. The documents may come from teaching and research institutions in France or abroad, or from public or private research centers.

L'archive ouverte pluridisciplinaire **HAL**, est destinée au dépôt et à la diffusion de documents scientifiques de niveau recherche, publiés ou non, émanant des établissements d'enseignement et de recherche français ou étrangers, des laboratoires publics ou privés.



PROF. EMMANUEL JACQUEMIN (Orcid ID : 0000-0002-7536-6272)

Editor: Emma Andersson

Article type : Original Articles

**Title: Functional rescue of an ABCB11 mutant by ivacaftor: a new targeted pharmacotherapy approach in bile salt export pump deficiency**

**Authors:** Elodie Mareux<sup>1,\*</sup>, Martine Lapalus<sup>1,\*</sup>, Rachida Amzal<sup>1</sup>, Marion Almes<sup>1,2</sup>, Tounsia Aït-Slimane<sup>3</sup>, Jean-Louis Delaunay<sup>3</sup>, Pauline Adnot<sup>1</sup>, Mauricette Collado-Hilly<sup>1</sup>, Anne Davit-Spraul<sup>1,4</sup>, Thomas Falguières<sup>1</sup>, Isabelle Callebaut<sup>5</sup>, Emmanuel Gonzales<sup>1,2,\*</sup>, Emmanuel Jacquemin<sup>1,2,\*</sup>

**Affiliations:**

<sup>1</sup>Université Paris-Saclay, Inserm, Physiopathogénèse et traitement des maladies du foie, UMR\_S 1193, Hepatinov, 91400 Orsay, France.

<sup>2</sup>Paediatric Hepatology & Paediatric Liver Transplant Department, Reference Center for Rare Paediatric Liver Diseases, FILFOIE, ERN RARE LIVER, Assistance Publique-Hôpitaux de Paris, Faculty of Medicine Paris-Saclay, CHU Bicêtre, 94270 Le Kremlin-Bicêtre, France.

<sup>3</sup>Sorbonne Université, Inserm, Centre de Recherche Saint-Antoine (CRSA), UMR\_S 938, Institute of Cardiometabolism and Nutrition (ICAN), 75012 Paris, France.

<sup>4</sup>Assistance Publique-Hôpitaux de Paris, CHU Bicêtre, Biochemistry Unit, 94270 Le Kremlin-Bicêtre, France.

<sup>5</sup>Sorbonne Université, Muséum National d'Histoire Naturelle, UMR CNRS 7590, Institut de Minéralogie, de Physique des Matériaux et de Cosmochimie, IMPMC, 75005 Paris, France.

\*equal contribution of the authors to the work.

**Corresponding author:** Pr Emmanuel Jacquemin, M.D., PhD., Service d'Hépatologie et de transplantation hépatique pédiatriques, Département de Pédiatrie, Centre Hospitalier Universitaire de Bicêtre, 78 rue du Général Leclerc, 94275 Le Kremlin-Bicêtre cedex, France. Tel: 33-1-45-21-31-68. Fax: 33-1-45-21-28-16. E-mail: emmanuel.jacquemin@aphp.fr

This article has been accepted for publication and undergone full peer review but has not been through the copyediting, typesetting, pagination and proofreading process, which may lead to differences between this version and the [Version of Record](#). Please cite this article as [doi: 10.1111/LIV.14518](#)

This article is protected by copyright. All rights reserved

**Authorship statement:** EM, ML, EG and EJ conceived and designed the study. EM, ML, RA, PA and IC carried out the experiments with contributions from MA, TAS, JLD, MCH and ADS. EM, ML, EG and EJ wrote the manuscript and designed the figures with input from all authors. TF contributed to the revision of the manuscript. All the authors contributed to data analyses, interpretation of the data, critical reviewing of the manuscript and approved the final version of the manuscript.

**Text electronic word count:** 4296

Figures: 4

Supporting information: 3 figures

**Abbreviations:** ABC, ATP-binding cassette; ATP, adenosine triphosphate; BA, bile acid; BSEP/Bsep, bile salt export pump; CFTR, cystic fibrosis transmembrane conductance regulator; GFP, green fluorescent protein; MDCK, Madin-Darby canine kidney; MDR3, multidrug resistance protein 3; MSD, membrane spanning domain; NBD, nucleotide binding domain; Ntcp, Na-taurocholate cotransporting polypeptide; PFIC2, progressive familial intrahepatic cholestasis type 2; TC, taurocholate; wt, wild type.

**Conflict of interest:** None

**Financial support:** EM was supported by « Ministère de l'Enseignement supérieur, de la Recherche et de l'innovation » (Paris, France). RA was supported by « Association pour la Recherche en Hépatologie Pédiatrique » (Hôpital Bicêtre, France) and by « Association Maladie Foie Enfants » (Malakoff, France). MA was supported by « Société Française de Pédiatrie » (Paris, France).

**Acknowledgements:** We thank AMFE (Association Maladie Foie Enfants, Malakoff, France), MLD (Monaco Liver disorder, Monaco), Association “Pour Louis 1000 Foie Merci” (Fournet-Luisans, France), Association “Il était un foie” (Plouescat, France) and Fondation Rumsey-Cartier (Genève, Switzerland) for their support and Professor Catherine Guettier (Pathology Unit, CHU Bicêtre, France) for performing immunostaining studies in patient liver. We thank Sylvie Fabrega (Viral Vector for Gene Transfer core facility of Structure Fédérative de Recherche Necker, University of Paris Descartes, Paris, France) for the preparation of lentiviral particles, and Rodolphe Auger (I2BC, CEA, CNRS, Université Paris-Saclay, Gif-sur-Yvette, France), and Brigitte Grosse (Université Paris-Saclay, Inserm, Physiopathogénèse et traitement

des maladies du foie, UMR\_S 1193, HepatinoV, 91400 Orsay, France) for technical support, as well as Pascale Dupuis-Williams (Université Paris-Saclay, Inserm, Physiopathogénèse et traitement des maladies du foie, UMR\_S 1193, HepatinoV, 91400 Orsay, France) for critical reading of the manuscript.

Accepted Article

## Abstract

**Background & Aim:** The canalicular bile salt export pump (BSEP/*ABCB11*) of hepatocytes is the main adenosine triphosphate (ATP)-binding cassette (ABC) transporter responsible for bile acid secretion. Mutations in *ABCB11* cause several cholestatic diseases, including progressive familial intrahepatic cholestasis type 2 (PFIC2) often lethal in absence of liver transplantation. We investigated *in vitro* the effect and potential rescue of a BSEP mutation by ivacaftor, a clinically approved cystic fibrosis transmembrane conductance regulator (CFTR/*ABCC7*) potentiator.

**Methods:** The p.T463I mutation, identified in a PFIC2 patient and located in a highly conserved ABC transporter motif, was studied by 3D structure modeling. The mutation was reproduced in a plasmid encoding a rat Bsep-green fluorescent protein. After transfection, mutant expression was studied in Can 10 cells. Taurocholate transport activity and ivacaftor effect were studied in Madin-Darby canine kidney (MDCK) clones co-expressing the rat sodium-taurocholate co-transporting polypeptide (*Ntcp/Slc10A1*).

**Results:** As the wild-type protein, Bsep<sup>T463I</sup> was normally targeted to the canalicular membrane of Can 10 cells. As predicted by 3D structure modeling, taurocholate transport activity was dramatically low in MDCK clones expressing Bsep<sup>T463I</sup>. Ivacaftor treatment increased by 1.7-fold taurocholate transport activity of Bsep<sup>T463I</sup> ( $p < 0.0001$ ), reaching 95% of Bsep<sup>wt</sup> activity. These data suggest that the p.T463I mutation impairs ATP-binding, resulting in Bsep dysfunction that can be rescued by ivacaftor.

**Conclusion:** These results provide experimental evidence of ivacaftor therapeutic potential for selected patients with PFIC2 caused by *ABCB11* missense mutations affecting BSEP function. This could represent a significant step forward for the care of patients with BSEP deficiency.

**Abstract electronic word count:** 249

**Keywords:** PFIC2, VX-770, potentiator, ABC transporters superfamily, cholestatic liver diseases, pediatrics.

## Lay summary

- Mutations in *ABCB11*/BSEP cause or predispose to several liver disorders, the most severe form being progressive familial intrahepatic cholestasis type 2 (PFIC2).
- More than half of PFIC2 patients do not or poorly respond to medical treatment and/or surgical biliary diversion and require liver transplantation.

- Our *in vitro* study shows that the p.T463I mutation of BSEP, identified in a PFIC2 patient, leads to a defect of canalicular bile acid transport activity and that ivacaftor, a clinically approved potentiator, can rescue this functional defect.
- This proof of concept suggests that ivacaftor might constitute an efficient targeted pharmacotherapy approach for some selected PFIC2 patients carrying *ABCB11* mutations that impairs BSEP function. This could represent a significant step forward for the care of patients with BSEP deficiency.

## Introduction

Numerous studies have shown that mutations in the *ABCB11* gene, encoding the bile salt export pump (BSEP), are associated with several cholestatic diseases of hepatocellular origin, the most severe form being progressive familial intrahepatic cholestasis type 2 (PFIC2).<sup>1,2</sup> BSEP is expressed at the canalicular membrane of hepatocytes and is the main ATP-binding cassette (ABC) transporter responsible for bile acid (BA) secretion.<sup>1</sup> As other members of the superfamily of ABC transporters, BSEP is characterized by two membrane-spanning domains (MSDs) involved in substrate specificity and export, and two nucleotide-binding domains (NBDs) providing the energy to pump substrates across the membrane against their electrochemical gradients.<sup>2,3</sup> In PFIC2, impaired biliary BA secretion leads to decreased bile flow, BA accumulation in hepatocytes, ongoing hepatocellular damage and increased risk of hepatocellular carcinoma. Clinical signs of cholestasis usually appear within the first year of life with jaundice and pruritus. Medical therapy with ursodeoxycholic acid (UDCA) and surgical therapy such as biliary diversion may provide some symptomatic relief. Nevertheless, in the majority of cases, liver transplantation is required before adulthood because of unremitting pruritus, hepatic failure or hepatocellular carcinoma. Numerous PFIC2-causing *ABCB11* mutations have been reported, mostly nonsense, missense and splicing mutations, but also small insertions, deletions and duplications.<sup>2,4-7</sup> Regarding the missense mutations, some of them affect the processing or trafficking of the protein, thereby causing its retention in the endoplasmic reticulum and subsequent mistargeting to the canalicular membrane. We have previously shown that 4-phenylbutyrate, a clinically approved pharmacological chaperone drug could rescue mistrafficking of some BSEP missense mutants.<sup>8,9</sup> Other *ABCB11* missense mutations, especially those involving the NBDs, lead to a correctly targeted protein whose BA transport activity is impaired.<sup>2,5</sup> In two major series reporting on 165 *ABCB11* mutations identified in patients with severe BSEP deficiency, 90 (55 %) were missense mutations including 44 (27%) that were located in the NBDs.<sup>4,7</sup> NBDs are well conserved throughout the ABC superfamily and contain specific motifs involved in ATP-binding and/or hydrolysis, such as the Walker-A and Walker-B motifs, the A-, D-, H-, and Q-loops, and the LSGGQ (Leu-Ser-Gly-Gly-Gln) signature which is unique to the ABC superfamily.<sup>3</sup> Ivacaftor (VX-770, Kalydeco®, Vertex Pharmaceuticals, Boston, MA) is a clinically approved potentiator treatment for some class III CFTR (cystic fibrosis transmembrane conductance regulator, *ABCC7*) mutations which are mainly located in the NBDs.<sup>10,11</sup> Interestingly, it has been shown that ivacaftor could also increase the function of some MDR3

(multidrug resistance protein 3, *ABCB4*) mutants resulting from mutations located in NBDs and responsible for PFIC3, another chronic cholestatic liver disease.<sup>12</sup> However, the ability of potentiators to increase the function of BSEP mutants affecting BA transport activity has not been studied. BSEP ATP-binding sites having a strong similarity with those of CFTR and MDR3, we selected the p.T463I mutation, identified in a PFIC2 patient and located in the Walker-A motif of the first BSEP nucleotide binding domain (NBD1). Herein, we report that the p.T463I mutant is correctly located at the canalicular membrane of hepatocytes but that its BA transport activity is decreased and that ivacaftor can rescue this functional defect.

## Materials and methods

### Patient's data and molecular modeling

The patient harboring the p.T463I mutation was referred to the pediatric hepatology unit of Bicêtre Hospital at age nine months. *ABCB11* gene analysis, liver immunohistochemistry using anti-human BSEP and MDR3 antibodies and analyses of bile composition were performed as previously reported.<sup>6</sup> Liver samples were obtained from the Centre de Ressources Biologiques des Hôpitaux Universitaires Paris-Saclay, France. Informed consent was obtained from the parents and this study protocol conformed to the ethical guidelines of the 1975 Declaration of Helsinki as reflected in a priori approval by the institution's human research committee (Comité de Protection des Personnes, Hôpital Bicêtre, Le Kremlin-Bicêtre, France). Model of the 3D structure of the *ABCB11* NBD1/NBD2 assembly was built with Modeller v9.15<sup>13</sup> using as a template the experimental structure of the MJ0796 NBD1/NBD2 heterodimer in complex with ATP (pdb 1l2t),<sup>14</sup> solved at 1.9 Å, as described previously for the modeling of the *ABCB4* NBD1/NBD2 assembly.<sup>12</sup> We have used this MJ0796 3D structure, rather than other 3D structures sharing higher sequence similarities with *ABCB11*, because of the high resolution observed within the ATP-binding sites. The sequence alignment used for modeling is given in Supporting Fig. S1.

### DNA constructs and mutagenesis

The plasmid pEGFP-N1 encoding a rat wild type (wt) Bsep-green fluorescent protein (GFP) fusion protein was a gift from J.L Boyer (Yale University School of Medicine, New Haven, CT).<sup>15</sup> Patient's mutation c.1388 C>T, p.T463I was introduced using the QuikChange Lightning Site-Directed Mutagenesis kit (Agilent Technologies, Massy, France) according to the manufacturer's instructions. The primers used for mutagenesis were 5'-AGTGGGGCTGGGAAGAGTATAGCATTACAGCTC-3' (forward) and 5'-GAGCTGTAATGCTATACTCTTCCCAGCCCCACT-3' (reverse). Rat Bsep was used because of its high degree of homology with its human ortholog and a higher level of expression in cultured cells.<sup>16</sup> Furthermore, the p.T463I mutation is located in a highly conserved region between human BSEP and rat Bsep. The whole construct was verified by Sanger sequencing.

### Cell culture and transfection

Can 10 cells were transiently transfected with the plasmids encoding Bsep-GFP (wt or T463I), as described.<sup>8,9</sup> This well characterized rat hepatocellular polarized line expresses only minimal level of Bsep and forms bile canaliculi, thus allowing the study of the subcellular localization of Bsep mutants.<sup>8,9,17</sup> Madin-Darby canine kidney (MDCK) cells, a well-characterized polarized kidney

cell line allowing measurement of Ntcp- and Bsep-mediated bile acid vectorial transport,<sup>18,19</sup> were transfected with the plasmids encoding Bsep-GFP (wt or T463I) using Fugene HD transfection reagent (Promega, Madison, WI), according to the manufacturer's instructions. Stable transfected clones were obtained by selection with 600 µg/mL G418 (Sigma-Aldrich Chimie, Lyon, France) for 3 weeks and were subsequently grown in the presence of 300 µg/mL G418, then sorted by limiting dilution.

#### ***Immunofluorescence and confocal microscopy***

Immunofluorescence analyses were performed as described.<sup>8,9</sup> For Can 10 cells, primary antibodies were a mouse anti-GFP (1:80; Roche Diagnostics, Meylan, France) and a rat anti-zonula occludens 1 (undiluted; a gift from B.R Stevenson<sup>20</sup>, Edmonton, Alberta, Canada). For confluent MDCK clones, primary antibodies were a rabbit anti-GFP (1:500; Abcam, Cambridge, UK), a mouse anti-cMyc (1:250; BD Pharmingen, San Diego, CA) and the rat anti-zonula occludens 1 (see above). Appropriate goat anti-immunoglobulin G Alexa Fluor 488 and Alexa Fluor 594 secondary antibodies (1:500; Molecular Probes, Eugene, OR) were used as described.<sup>8,9</sup> The coverslips, embedded in mounting medium containing DAPI (Sigma-Aldrich Chimie, Lyon, France), were examined with a confocal microscope (Eclipse TE-2000-Nikon-C1) equipped with 60 x objective and serial *xy* optical sections with a *z*-step of 0.3 µm were taken using NIS-Elements software (Nikon).

#### ***Quantification of cells targeting Bsep to the canalicular pole***

Can 10 cells expressing Bsep-GFP (wt or T463I) and forming bile canaliculi were examined by epifluorescence microscopy. Bile canaliculi were identified by phase contrast and by immunolocalization of ZO-1 (at the seal of bile canaliculi). Among Bsep-GFP-positive Can 10 cells forming canaliculi, the percentage of cells expressing Bsep-GFP at the canalicular membrane was determined (40-100 cells were examined per coverslip, two coverslips were used per culture and three independent cultures of Can 10 cells were performed).

#### ***Expression of Ntcp in MDCK Bsep expressing clones***

The rat cDNA of the sodium-taurocholate co-transporting polypeptide (Ntcp/*Slc10A1*) was cloned into the lentiviral vector pLenti-cMyc-DDK-IRES-Puro (PS100069, OriGene, Rockville, MD). The MDCK clones with the highest Bsep-GFP (wt or T463I) expression and parental MDCK cells were infected with lentiviral particles containing the recombined plasmid at a multiplicity of infection of 30 and recombinant cells were selected with 3 µg/mL of puromycin (Ozyme, Paris, France).

### ***Immunoblot analyses***

Cell lysates from cultured MDCK clones and immunoblotting were performed as described<sup>21</sup> using mouse anti-GFP (1:500; Roche Diagnostics, Meylan, France), anti-cMyc (1:500; BD Pharmigene, San Diego, CA) and anti- $\beta$ -actin (1:3000, Sigma Aldrich, Saint-Louis, MO) antibodies incubated overnight in PBS with 0.05 % tween followed by horseradish peroxidase-linked mouse-specific secondary antibodies (GE Healthcare, Little Chalfont, UK). Development of peroxidase activity was performed with an ECL detection kit (BioRad, Marnes-La-Coquette, France). Bsep-GFP, Ntcp-cMyc and  $\beta$ -actin electrophoretic patterns were separately quantified on gels using ImageJ software (U.S. National Institutes of Health, Bethesda, MD). Bsep-GFP and Ntcp-cMyc relative expressions were normalized to the expression of  $\beta$ -actin.

### ***Taurocholate transport assay and ivacaftor treatment***

Parental MDCK cells and MDCK clones stably expressing Bsep-GFP and/or Ntcp-cMyc were seeded on polyethylene terephthalate membrane inserts (pore size 3  $\mu$ m; Falcon, Bedford, MA) in 24-well plates at a density of  $10^4$  cells/insert. During the five following days, the integrity of cell monolayers was assessed by transepithelial electrical resistance measurements and Lucifer yellow permeability tests.<sup>22</sup> Culture medium was replaced by prewarmed transport buffer (in mM: 118 NaCl, 23.8 NaHCO<sub>3</sub>, 4.83 KCl, 0.96 KH<sub>2</sub>PO<sub>4</sub>, 1.2 MgSO<sub>4</sub>, 12.5 HEPES, 5 glucose, and 1.53 CaCl<sub>2</sub>, adjusted to pH 7.4) in apical and basal compartments, in the absence or presence of ivacaftor (Cliniscience, Nanterre, France). Ivacaftor was used at a concentration of 10  $\mu$ M, as previously reported for the rescue of class III CFTR and MDR3 mutants.<sup>10,12</sup> Taurocholate (TC, 0.9  $\mu$ M, Sigma-Aldrich, Saint Louis, MO) and [<sup>3</sup>H]Taurocholate ([<sup>3</sup>H]TC, 0.1  $\mu$ M, 1  $\mu$ Ci/mL, Perkin Elmer, Waltham, MA) were added in the basal compartment.<sup>19</sup> After two hours, the apical buffer was collected, membrane inserts were washed with ice-cold PBS, then cells were lysed with 120  $\mu$ L 1% Triton X-100. Transcellular transport and intracellular accumulation of [<sup>3</sup>H]TC were calculated from the radioactivity measured by scintillation counter (Hidex 300 SL, Hidex Turku, Finland) in the apical buffer and cell lysates, respectively. Aliquots (50  $\mu$ L) of cell lysates were used to determine protein concentration (DC Protein Assay Kit, BioRad, Marnes-La-Coquette, France), with bovine serum albumin as a standard. Transport data were normalized to protein amount.

### ***Statistical analyses***

Data are expressed as means  $\pm$  standard error of the mean (SEM). Statistical analyses were performed using ANOVA, except for the quantification of canalicular Bsep-GFP positive Can 10

cells which was analyzed using the Student  $t$  test. A  $p$  value  $< 0.05$  was considered to be significant.

Accepted Article

## Results

### *The p.T463I mutation of BSEP and 3D structure modeling of human BSEP NBDs*

The p.T463I missense mutation of BSEP was identified in one allele of *ABCB11* in a PFIC2 patient harboring the p.R1057X nonsense mutation in the other allele.<sup>4,5,7,23</sup> This nonsense mutation leads to the introduction of a premature termination codon in NBD2 and predicts premature truncation of BSEP, resulting in the absence of protein synthesis through a nonsense-mediated mRNA decay process.<sup>23</sup> Immunostaining of the liver from this patient revealed a faint but positive canalicular staining of BSEP, as compared to the normal human liver (Fig. 1A-B), without alteration of the MDR3 staining (Fig. 1C-D). Moreover, biliary BA concentration in this patient was low (1 mM, N > 10).<sup>6</sup> Therefore, it is likely that the positive canalicular BSEP immunostaining observed in the liver of the patient is due to normal canalicular targeting of the BSEP<sup>T463I</sup> mutant.

BSEP consists of 1321 amino acids distributed in a tandemly duplicated structure composed of two MSDs (MSD1 and MSD2) and two cytoplasmic NBDs (NBD1 and NBD2). There are two composite ATP-binding sites formed at the interface of the head-to-tail NBD1/NBD2 heterodimer (site A and B). Each site is indeed composed of Walker-A/Walker-B motifs from one NBD and the signature motif of the other NBD (Fig. 2A). In contrast to MDR3, BSEP has asymmetric ATP-binding sites, one of them (site A) being degenerate with the following distinctive amino acids: Y429 (A loop), K461-S462 (Walker A), Q503 (Q loop), M584 (Walker B), H615 (H-loop), L1219-S1220-R1221-G1222-E1223 (ABC signature) (Fig. 2). As for other asymmetric ABC transporters, it is expected that this site is catalytically inactive, with long-term ATP-binding at the NBD interface.<sup>24</sup> The p.T463I missense mutation is located within the Walker-A motif of NBD1 and belongs to the degenerate site A. The 3D structure modeling predicts that this residue interacts with the ATP  $\alpha$ -phosphate (Fig. 2B). Its substitution is thus expected to prevent or disturb ATP-binding, hindering ATP-induced NBDs dimerization and resulting in BSEP dysfunction.

### *Subcellular localization of Bsep<sup>T463I</sup> in Can 10 cells*

Localization of Bsep<sup>T463I</sup> was compared to that of Bsep<sup>wt</sup> in Can 10 cells after transient Bsep-GFP expression. As the wt protein, Bsep<sup>T463I</sup> was located at the canalicular membrane, delineated by the tight junction-associated protein ZO-1 (Fig. 3A). Quantification showed that all Bsep-GFP-positive Can 10 cells forming canaliculi expressed Bsep (wt or T463I) exclusively at the canalicular membrane (Fig. 3B). These observations indicate that the p.T463I mutation did not impair the intracellular trafficking of Bsep.

### ***Generation of MDCK clones stably expressing Bsep and Ntcp***

The Bsep-mediated BA secretion was evaluated in MDCK clones stably expressing Bsep-GFP (wt or T463I) and/or Ntcp-cMyc. The latter is a basolateral transporter allowing BA entry into MDCK cells. It is also important to note that MDCK cells are reported not to endogenously express Bsep.<sup>19,25</sup> The appropriate expressions of Bsep and Ntcp, at the apical and basolateral membrane of MDCK cells respectively, were checked using immunodetection techniques and confocal imaging. On immunoblotting, Bsep-GFP (apparent molecular mass of 190 kDa) was detected in MDCK-Bsep<sup>wt</sup>, MDCK-Bsep<sup>wt</sup>/Ntcp and MDCK-Bsep<sup>T463I</sup>/Ntcp clones (Fig. 4A and Supporting Fig. S2A). The expression of Ntcp-cMyc was detected at 53 kDa in MDCK-Ntcp, MDCK-Bsep<sup>wt</sup>/Ntcp and MDCK-Bsep<sup>T463I</sup>/Ntcp clones (Fig. 4A and Supporting Fig. S2B). Quantification of Bsep-GFP and Ntcp-cMyc electrophoretic patterns displayed expression levels of Bsep-GFP and Ntcp-cMyc among MDCK clones that were not statistically different except for MDCK-Ntcp clone that, as expected, did not express Bsep-GFP (Fig. 4, B and C). The subcellular localization of Bsep (wt or T463I) and Ntcp was assessed using confocal microscopy. Bsep (wt and T463I) were predominantly located along the apical membrane of MDCK-Bsep<sup>wt</sup>, MDCK-Bsep<sup>wt</sup>/Ntcp and MDCK-Bsep<sup>T463I</sup>/Ntcp cells (Fig. 4D and Supporting Fig. S2C). This localization is consistent with the normal canalicular location of Bsep<sup>T463I</sup> observed in Can 10 cells (Fig. 3A) and in the patient's liver (Fig. 1B). As expected, Ntcp was exclusively located at the basolateral membrane in MDCK-Ntcp, MDCK-Bsep<sup>wt</sup>/Ntcp and MDCK-Bsep<sup>T463I</sup>/Ntcp clones (Fig. 4D and Supporting Fig. S2C). Control parental MDCK cells did not express detectable amounts of Bsep-GFP or Ntcp-cMyc on immunoblotting and on confocal imaging (Supporting Fig. S2, A, B and C).

### ***BA transport activity of Bsep<sup>T463I</sup> and effect of ivacaftor***

The BA transport activity and the effect of ivacaftor were assessed in MDCK clones stably expressing Bsep-GFP (wt or T463I) and/or Ntcp-cMyc by measuring the intracellular [<sup>3</sup>H]TC accumulation and the transcellular transport of [<sup>3</sup>H]TC across the monolayers. As previously reported,<sup>19</sup> intracellular [<sup>3</sup>H]TC concentration in MDCK clone expressing only Bsep<sup>wt</sup> was minimal, whereas in MDCK-Ntcp clone, it was significantly higher indicating that Ntcp expression is required for the entry of TC into cells (Supporting Fig. S2D). In addition, the transcellular transport of [<sup>3</sup>H]TC in the apical direction and through the apical membrane was 10.8-fold higher in MDCK-Ntcp clone compared with MDCK-Bsep<sup>wt</sup> clone, suggesting the presence of an apical transporter other than Bsep that carries TC in MDCK cells (Supporting Fig. S2E), as previously reported.<sup>19</sup> The basal to apical flux of [<sup>3</sup>H]TC was 3.5-fold higher and

intracellular [<sup>3</sup>H]TC concentration was 7-fold lower compared with MDCK-Ntcp clone, indicating that Bsep<sup>wt</sup> efficiently transports TC across the apical membrane (Supporting Fig. S2, D and E). Thus, our experimental model allows a precise measurement of BA uptake and export through Ntcp and Bsep transporters, respectively. The Bsep<sup>T463I</sup> mutant likely retains residual transport activity since the intracellular [<sup>3</sup>H]TC concentration in MDCK-Bsep<sup>T463I</sup>/Ntcp clone was significantly lower ( $p < 0.0001$ ) than in MDCK-Ntcp clone ( $42.2 \pm 3.8$  vs  $104.0 \pm 12.5$  pmol/mg protein, respectively) and the [<sup>3</sup>H]TC transcellular transport detected in MDCK-Bsep<sup>T463I</sup>/Ntcp clone was significantly higher ( $p = 0.0015$ ) than the one measured in the MDCK-Ntcp clone ( $177.2 \pm 8.7$  vs  $87.4 \pm 5.1$  pmol/mg protein, respectively; Fig. 4, E and F). However, we observed a marked increase of intracellular [<sup>3</sup>H]TC concentration by 2.9-fold ( $p < 0.0001$ ) in MDCK-Bsep<sup>T463I</sup>/Ntcp clone compared with MDCK-Bsep<sup>wt</sup>/Ntcp clone and the amount of [<sup>3</sup>H]TC detected at the apical compartment was dramatically decreased ( $p < 0.0001$ ), approaching 58 % of the transcellular transport measured in MDCK-Bsep<sup>wt</sup>/Ntcp clone (Fig. 4, E and F). These observations indicate that the BA transport activity of Bsep<sup>T463I</sup> is impaired. No significant effect of treatment with ivacaftor (10  $\mu$ M) was observed neither on the morphology of the cells and the distribution of Bsep-GFP or Ntcp-cMyc (Supporting Fig. S3) nor on BA transport activity in MDCK-Ntcp and MDCK-Bsep<sup>wt</sup>/Ntcp clones ( $p > 0.9999$ ; Fig. 4, E and F). In MDCK-Bsep<sup>T463I</sup>/Ntcp clone, ivacaftor significantly decreased ( $p = 0.0449$ ) intracellular [<sup>3</sup>H]TC concentration by 1.8-fold and significantly increased ( $p < 0.0001$ ) the transcellular transport of [<sup>3</sup>H]TC by 1.6-fold, reaching 95 % of the Bsep<sup>wt</sup> transport activity (Fig. 4, E and F).

## Discussion

The data presented here provide evidence that functional defect of a PFIC2-causing BSEP missense mutation could be rescued *in vitro* by ivacaftor. The p.T463I mutation was identified in a compound heterozygous patient with the p.R1057X nonsense mutation in the other allele of BSEP. Since PFIC2 is an autosomal recessive disease, the heterozygous p.R1057X nonsense mutation alone cannot be responsible for the clinical phenotype. Our hypothesis was that Bsep<sup>T463I</sup> was correctly targeted to the bile canaliculi, as we confirmed when expressed in Can 10 cells, but was not functional, as suggested by the low concentration of BA measured in patient's bile. However, Bsep<sup>T463I</sup> likely retains residual BA transport activity because the biliary BA concentration was not decreased as much as usually observed in PFIC2 patients.<sup>6</sup> This is in line with our measurements of BA transport activity in MDCK-Bsep<sup>T463I</sup>/Ntcp cells.

The p.T463I mutation occurs in the Walker-A motif of NBD1, a region highly conserved throughout the vertebrate phylum and therefore likely containing essential residues for BSEP function.<sup>26</sup> In agreement with these observations, structure modeling predicted that p.T463I mutation disrupted interaction with the ATP  $\alpha$ -phosphate and thereby altered ATP-induced NBD dimerization, which is critical for BA transport function.<sup>14</sup> We show that, although correctly targeted to the canalicular membrane, Bsep<sup>T463I</sup> displayed a major activity defect. So far, no targeted pharmacotherapy has been proposed for mutations that affect BSEP function. Ivacaftor, a small molecule identified by high-throughput screening, was clinically approved by FDA and EMA for some class III CFTR mutations that impaired normal channel gating activity. Ivacaftor treatment has been shown to be safe when used in cystic fibrosis patients and leads to a significant improvement in respiratory function.<sup>11,27</sup> Furthermore, ivacaftor rescued *in vitro* the functional defect of class III MDR3 missense mutants involving the NBDs.<sup>12</sup> Considering the motif conservation and structure-function relationships between BSEP, CFTR and MDR3, we show here that ivacaftor can also correct the functional defect of Bsep<sup>T463I</sup> mutant. This mutant was previously reported in two families.<sup>4,5</sup> As mentioned earlier, about a quarter of *ABCB11* mutations identified in patients with severe BSEP deficiency are missense mutations located in the NBDs.<sup>4,7</sup> Thereby, this category of patients might be good candidates for ivacaftor treatment, provided that results of 3D structure analyses and *in vitro* studies are supportive.

The mechanism of action of ivacaftor remains largely unknown. Concerning CFTR, cryo-electron microscopy has recently revealed, a potential ivacaftor binding site within the MSDs.<sup>28</sup> It has been proposed that the binding of ivacaftor shifts the gating transitions towards the open state of the

channel, regardless of the dimerization state of the NBDs and in an ATP-independent manner.<sup>28-30</sup> On another hand, a research team has proposed an ATP-dependent mechanism for ivacaftor potentiation<sup>31</sup> and, more recently, demonstrated a clear dependence on the phosphorylation state.<sup>32</sup> Ivacaftor has also been shown to stimulate the ATPase activity of PgP (*ABCB1*), probably causing a stabilization of the protein.<sup>33</sup> A similar mechanism could be proposed for Bsep, in which the drug would stabilize the MSDs in a substrate binding competent conformational state. Further studies are needed to gain insights into these mechanisms and to define its potential ATP-dependency.

Our findings show that deficient BA secretion activity due to a missense *ABCB11* mutation can be rescued *in vitro* by the CFTR potentiator, ivacaftor. These results provide experimental evidence that ivacaftor may offer a new therapeutic option for selected patients with BSEP deficiency due to missense mutations located in the NBDs. Studies in selected PFIC2 patients are warranted to confirm the beneficial effect of ivacaftor. In addition, in PFIC2 patients, the combination of ivacaftor with a chaperone drug could be an interesting option to improve the functional level of BSEP mutants retargeted by a chaperone drug to the bile canaliculus, as it has been proposed for selected cystic fibrosis patients.<sup>8,9,34</sup>

## References

Author names in bold designated shared co-first authorship.

1. Davit-Spraul A, Gonzales E, Baussan C, Jacquemin E. Progressive familial intrahepatic cholestasis. *Orphanet J Rare Dis.* 2009;4:1.
2. Soroka CJ, Boyer JL. Biosynthesis and trafficking of the bile salt export pump, BSEP: therapeutic implications of BSEP mutations. *Mol Aspects Med.* 2014;37:3-14.
3. Dean M, Rzhetsky A, Allikmets R. The human ATP-binding cassette (ABC) transporter superfamily. *Genome Res.* 2001;11(7):1156-1166.
4. Strautnieks SS, Byrne JA, Pawlikowska L, et al. Severe bile salt export pump deficiency: 82 different ABCB11 mutations in 109 families. *Gastroenterology.* 2008;134(4):1203-1214.
5. Byrne JA, Strautnieks SS, Ihrke G, et al. Missense mutations and single nucleotide polymorphisms in ABCB11 impair bile salt export pump processing and function or disrupt pre-messenger RNA splicing. *Hepatology.* 2009;49(2):553-567.
6. Davit-Spraul A, Fabre M, Branchereau S, et al. ATP8B1 and ABCB11 analysis in 62 children with normal gamma-glutamyl transferase progressive familial intrahepatic cholestasis (PFIC): phenotypic differences between PFIC1 and PFIC2 and natural history. *Hepatology.* 2010;51(5):1645-1655.
7. Droge C, Bonus M, Baumann U, et al. Sequencing of FIC1, BSEP and MDR3 in a large cohort of patients with cholestasis revealed a high number of different genetic variants. *J Hepatol.* 2017;67(6):1253-1264.
8. Gonzales E, Grosse B, Cassio D, Davit-Spraul A, Fabre M, Jacquemin E. Successful mutation-specific chaperone therapy with 4-phenylbutyrate in a child with progressive familial intrahepatic cholestasis type 2. *J Hepatol.* 2012;57(3):695-698.
9. Gonzales E, Grosse B, Schuller B, et al. Targeted pharmacotherapy in progressive familial intrahepatic cholestasis type 2: Evidence for improvement of cholestasis with 4-phenylbutyrate. *Hepatology.* 2015;62(2):558-566.
10. Van Goor F, Hadida S, Grootenhuys PD, et al. Rescue of CF airway epithelial cell function in vitro by a CFTR potentiator, VX-770. *Proc Natl Acad Sci U S A.* 2009;106(44):18825-18830.
11. De Boeck K, Munck A, Walker S, et al. Efficacy and safety of ivacaftor in patients with cystic fibrosis and a non-G551D gating mutation. *J Cyst Fibros.* 2014;13(6):674-680.

12. **Delaunay JL, Bruneau A, Hoffmann B, et al.** Functional defect of variants in the adenosine triphosphate-binding sites of ABCB4 and their rescue by the cystic fibrosis transmembrane conductance regulator potentiator, ivacaftor (VX-770). *Hepatology*. 2017;65(2):560-570.
13. Webb B, Sali A. Protein Structure Modeling with MODELLER. *Methods Mol Biol*. 2017;1654:39-54.
14. Smith PC, Karpowich N, Millen L, et al. ATP binding to the motor domain from an ABC transporter drives formation of a nucleotide sandwich dimer. *Mol Cell*. 2002;10(1):139-149.
15. Lam P, Pearson CL, Soroka CJ, Xu S, Mennone A, Boyer JL. Levels of plasma membrane expression in progressive and benign mutations of the bile salt export pump (Bsep/Abcb11) correlate with severity of cholestatic diseases. *Am J Physiol Cell Physiol*. 2007;293(5):C1709-1716.
16. Wang L, Soroka CJ, Boyer JL. The role of bile salt export pump mutations in progressive familial intrahepatic cholestasis type II. *J Clin Invest*. 2002;110(7):965-972.
17. Cassio D, Macias RI, Grosse B, Marin JJ, Monte MJ. Expression, localization, and inducibility by bile acids of hepatobiliary transporters in the new polarized rat hepatic cell lines, Can 3-1 and Can 10. *Cell Tissue Res*. 2007;330(3):447-460.
18. Harris MJ, Kagawa T, Dawson PA, Arias IM. Taurocholate transport by hepatic and intestinal bile acid transporters is independent of FIC1 overexpression in Madin-Darby canine kidney cells. *Journal of gastroenterology and hepatology*. 2004;19(7):819-825.
19. Mita S, Suzuki H, Akita H, et al. Vectorial transport of bile salts across MDCK cells expressing both rat Na<sup>+</sup>-taurocholate cotransporting polypeptide and rat bile salt export pump. *Am J Physiol Gastrointest Liver Physiol*. 2005;288(1):G159-167.
20. Stevenson BR, Siliciano JD, Mooseker MS, Goodenough DA. Identification of ZO-1: a high molecular weight polypeptide associated with the tight junction (zonula occludens) in a variety of epithelia. *J Cell Biol*. 1986;103(3):755-766.
21. Bender V, Buschlen S, Cassio D. Expression and localization of hepatocyte domain-specific plasma membrane proteins in hepatoma x fibroblast hybrids and in hepatoma dedifferentiated variants. *J Cell Sci*. 1998;111 ( Pt 22):3437-3450.

22. Mahdi ZM, Synal-Hermanns U, Yoker A, Locher KP, Stieger B. Role of Multidrug Resistance Protein 3 in Antifungal-Induced Cholestasis. *Mol Pharmacol*. 2016;90(1):23-34.
23. Strautnieks SS, Bull LN, Knisely AS, et al. A gene encoding a liver-specific ABC transporter is mutated in progressive familial intrahepatic cholestasis. *Nat Genet*. 1998;20(3):233-238.
24. Csanady L. Degenerate ABC composite site is stably glued together by trapped ATP. *J Gen Physiol*. 2010;135(5):395-398.
25. Quan Y, Jin Y, Faria TN, et al. Expression Profile of Drug and Nutrient Absorption Related Genes in Madin-Darby Canine Kidney (MDCK) Cells Grown under Differentiation Conditions. *Pharmaceutics*. 2012;4(2):314-333.
26. **Cai SY, Wang L**, Ballatori N, Boyer JL. Bile salt export pump is highly conserved during vertebrate evolution and its expression is inhibited by PFIC type II mutations. *Am J Physiol Gastrointest Liver Physiol*. 2001;281(2):G316-322.
27. Pharmaceuticals Vertex. Annex I: summary of product characteristics: Kalydeco 150 mg film-coated tablets. 2017.  
[http://www.ema.europa.eu/docs/en\\_GB/document\\_library/EPAR\\_-\\_Product\\_Information/human/002494/WC500130696.pdf](http://www.ema.europa.eu/docs/en_GB/document_library/EPAR_-_Product_Information/human/002494/WC500130696.pdf)
28. Liu F, Zhang Z, Levit A, et al. Structural identification of a hotspot on CFTR for potentiation. *Science (New York, NY)*. 2019;364(6446):1184-1188.
29. Eckford PD, Li C, Ramjeesingh M, Bear CE. Cystic fibrosis transmembrane conductance regulator (CFTR) potentiator VX-770 (ivacaftor) opens the defective channel gate of mutant CFTR in a phosphorylation-dependent but ATP-independent manner. *J Biol Chem*. 2012;287(44):36639-36649.
30. Jih KY, Hwang TC. Vx-770 potentiates CFTR function by promoting decoupling between the gating cycle and ATP hydrolysis cycle. *Proc Natl Acad Sci U S A*. 2013;110(11):4404-4409.
31. Cui G, McCarty NA. Murine and human CFTR exhibit different sensitivities to CFTR potentiators. *Am J Physiol Lung Cell Mol Physiol*. 2015;309(7):L687-699.
32. Cui G, Stauffer BB, Imhoff BR, et al. VX-770-mediated potentiation of numerous human CFTR disease mutants is influenced by phosphorylation level. *Sci Rep*. 2019;9(1):13460.

33. Lingam S, Thonghin N, Ford RC. Investigation of the effects of the CFTR potentiator ivacaftor on human P-glycoprotein (ABCB1). *Sci Rep.* 2017;7(1):17481.
34. Wainwright CE, Elborn JS, Ramsey BW, et al. Lumacaftor-Ivacaftor in Patients with Cystic Fibrosis Homozygous for Phe508del CFTR. *N Engl J Med.* 2015.

## Figure legends

**Figure 1. Immunohistochemical detection of BSEP and MDR3 in the liver of the PFIC2 patient.** (A-B) BSEP staining (brown) in normal human liver (A) and patient liver (B). (C-D) MDR3 staining (brown) in normal human liver (C) and patient liver (D). Nuclei are also shown (blue). The livers display normal canalicular staining (A, C, D) and faint canalicular staining (B). Insets are magnified areas indicated by dashed squares. Original magnification: 250X. Bars: 50  $\mu\text{m}$ .

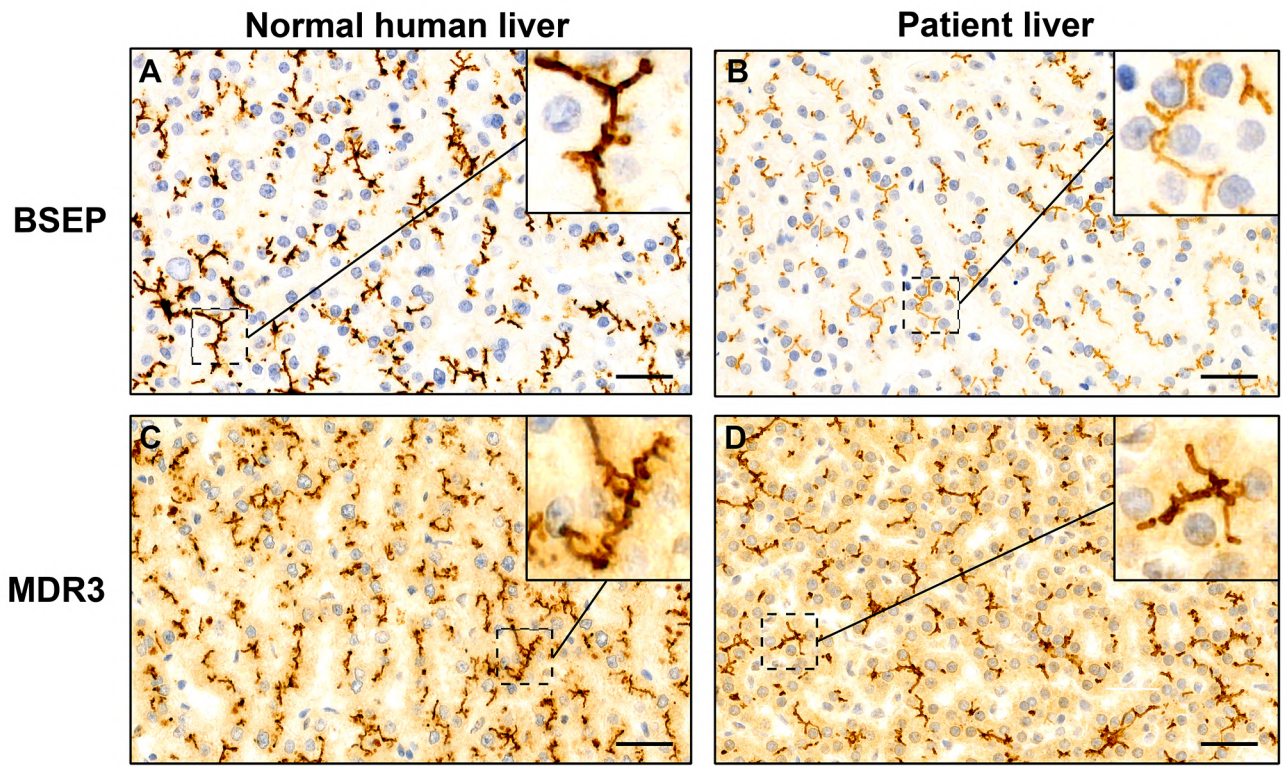
**Figure 2. Organization of human BSEP and 3D structure modeling of ATP-binding site A.** (A) The ATP-binding sites (site A and B) of BSEP are formed by the Walker-A (WA) and Walker-B (WB) motifs of one NBD and the ABC signature of the other NBD. The p.T463I mutation (in red) belongs to the WA motif of NBD1, within the degenerate ATP-binding site A. (B) View (ribbon representation) of the model of the 3D structure of BSEP degenerate ATP-binding site A, in which amino acid T463I (depicted in green with atomic details) is interacting with the ATP  $\alpha$ -phosphate (dashed lines).

**Figure 3. Immunolocalization of Bsep-GFP (wt and T463I) in transiently transfected Can 10 cells.** (A) Immunolocalization of Bsep<sup>wt</sup>-GFP, Bsep<sup>T463I</sup>-GFP (green) and tight junction protein zonula occludens 1 (ZO-1, red) in transiently transfected Can 10 cells using confocal microscopy. Dashed lines: transfected cells. Original magnification: 60X. \*Bile canaliculus. Bars: 10  $\mu\text{m}$ . (B) Quantification of experiments shown in A. Among Bsep-GFP-positive cells forming canaliculi, the percentage of cells expressing Bsep-GFP at the canalicular membrane was determined. *ns*: not significant (Student *t* test).

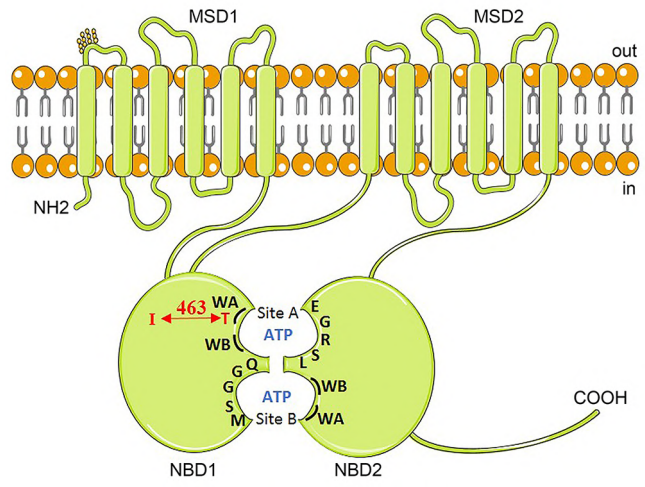
**Figure 4. Studies of Bsep-GFP (wt or T463I) and/or Ntcp-cMyc in stable MDCK clones and effect of ivacaftor.** (A) MDCK clones stably expressing Bsep-GFP (wt or T463I) and/or Ntcp-cMyc were lysed and analyzed by immunoblotting using anti-GFP and anti-cMyc antibodies. (B-C) Bsep-GFP (B) and Ntcp-cMyc (C) electrophoretic patterns from A were separately quantified and their relative amounts were calculated and normalized to  $\beta$ -actin. Results are means ( $\pm$  SEM) of at least three experiments. *ns*: not significant; \*\*  $p < 0.01$ ; \*\*\*  $p < 0.001$  (one-way ANOVA). (D) Immunolocalization by confocal microscopy of Bsep-GFP (wt or T463I) and Ntcp-cMyc, shown in green and red, respectively. Nuclei (blue) are shown in the merged pictures. *Bottom, center and right* panels show *x-z*, *x-y* and *y-z* plane images, respectively. Original magnification: 60X. Bars: 10  $\mu\text{m}$ . (E) Intracellular [<sup>3</sup>H]TC accumulation and (F) Vectorial transport of [<sup>3</sup>H]TC in MDCK clones expressing Ntcp, Bsep<sup>wt</sup>/Ntcp or Bsep<sup>T463I</sup>/Ntcp in the absence (-) or presence (+)

of ivacaftor (10  $\mu$ M). Results are means  $\pm$  SEM of at least three experiments per condition. *ns*: not significant; \*  $p < 0.05$ ; \*\*  $p < 0.01$ ; \*\*\*\*  $p < 0.0001$  (two-way ANOVA).

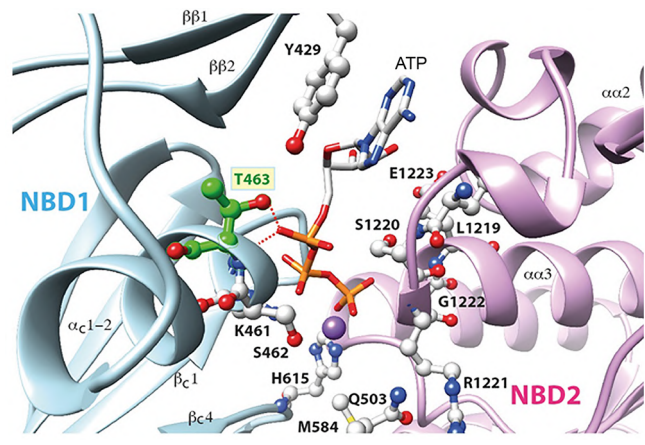
Accepted Article



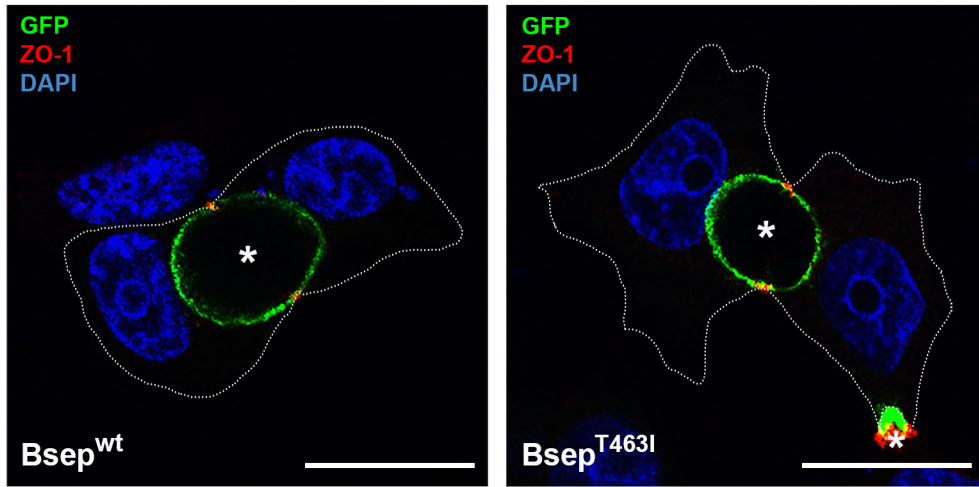
liv\_14518\_f1.tif



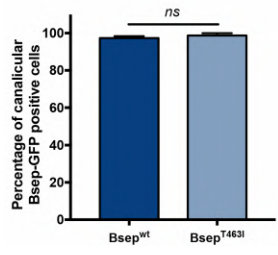
liv\_14518\_f2a.tif



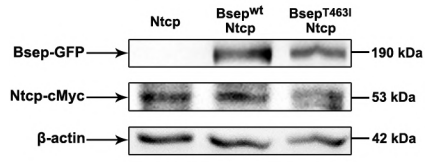
liv\_14518\_f2b.tif



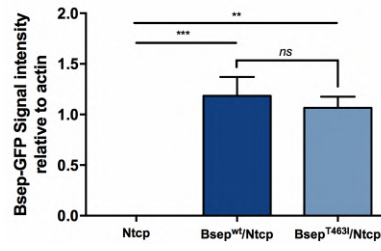
liv\_14518\_f3a.tif



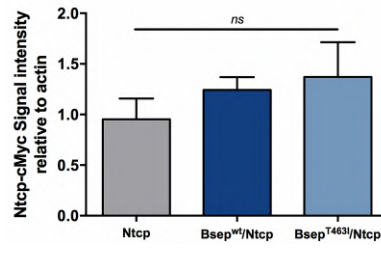
liv\_14518\_f3b.tif



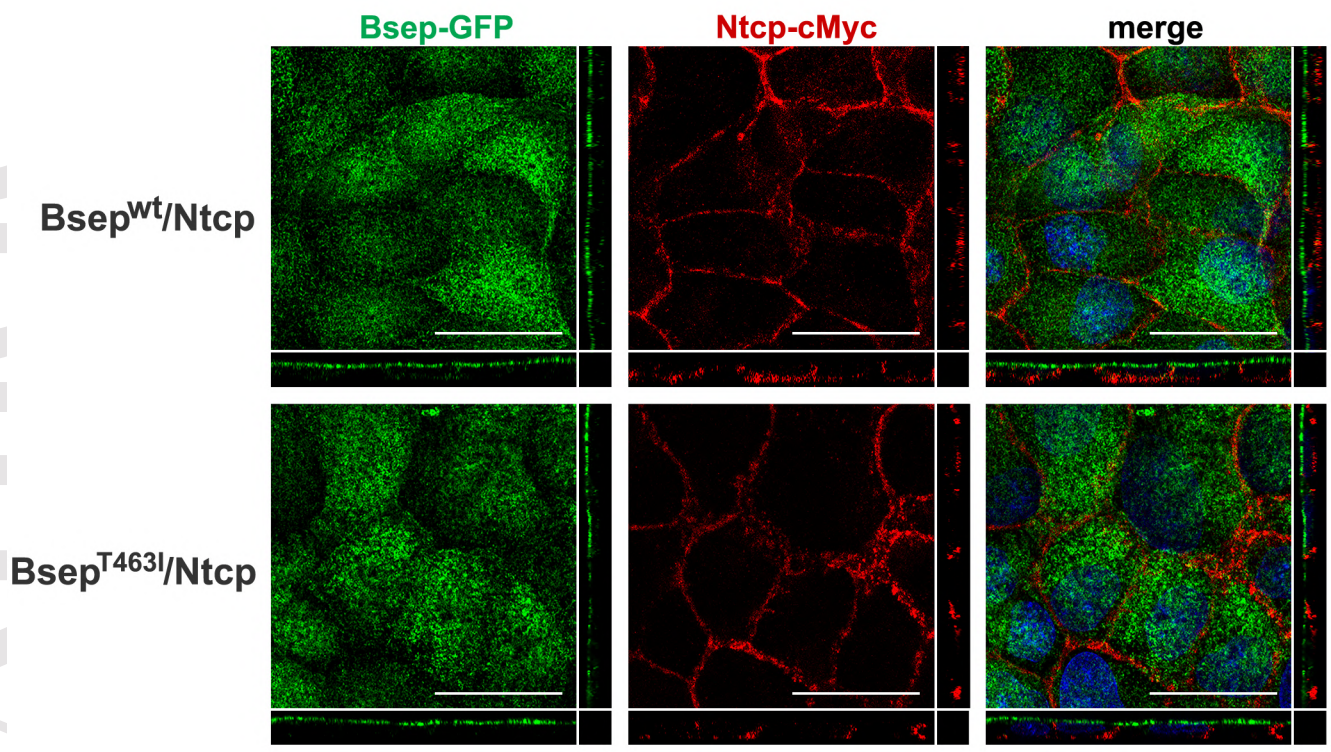
liv\_14518\_f4a.tif



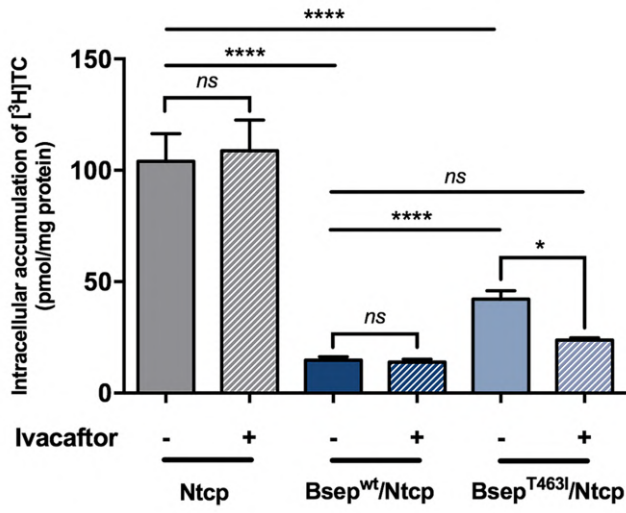
liv\_14518\_f4b.tif



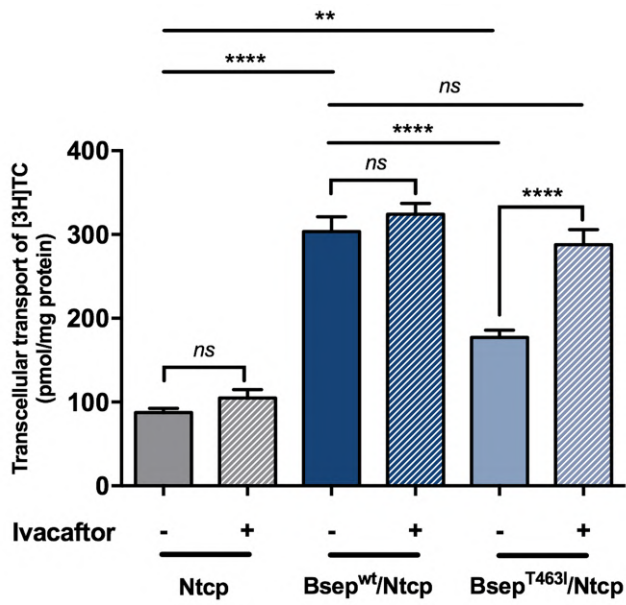
liv\_14518\_f4c.tif



liv\_14518\_f4d.tif



liv\_14518\_f4e.tif



liv\_14518\_f4f.tif